AXIAL IMPACT OF OPEN-SECTION TWCF COLUMNS – EXPERIMENTAL STUDY

MARIA KOTEŁKO[1], ARTUR MOŁDAWA[1] , MARCIN JANKOWSKI[2]

Abstract. The paper is devoted to the results of experimental study into the crushing behaviour of TWCF open section columns subjected to axial impact. Steel channel and top-hat section was under investigation. The paper contains a results summary of quasi-dynamic and dynamic impact tests performed on about 100 of those sections of different dimensions subjected to axial load of different velocities. Experimental quasi-dynamic tests were conducted on the testing machine with different loading velocities up to 600 mm/min. The impact tests were performed on the drop hammer rig with the impact energy up to 5 kJ and impact velocity up to 10 m/s. An influence of the column initial length and impact velocity on the crushing behaviour (failure mode) was investigated. Particularly, the critical length of the transition from progressive buckling to global bending failure mode and its dependence on section dimensions and the impact velocity was under investigation. Experimental results were compared with the results of the analytical calculations of critical (transition) buckling length based on the simplified analytical theoretical models. The results are presented in load-time and load-shortening diagrams and failure patterns. Some conclusions concerning the determination of critical buckling length, applicability of the theoretical models applied and an influence of the impact velocity upon the critical buckling length and final mode of failure related to the energy absorption capability of columns are derived.

Key words: thin-walled columns, open sections, impact, experiment

1. INTRODUCTION

Load-carrying capacity and energy absorption of TWCF subjected to dynamic loading is an important problem in two areas of engineering applications: first – energy absorption of members acting as energy absorbers during accidental collision of automotive or rail vehicles, secondly – load-carrying capacity of structural members subjected to seismic loads. The term 'dynamic crushing' is used in the present paper in the sense of progressive crushing of a structure subjected to the impulse of an applied load.

An effective design of energy absorbing TWCF structural member demands to determine a load-deformation relation of the member under impact load. In the

[1] Lódź University of Technology, Department of Strength of Materials, 90-924 Łódź, Stefanowskiego 1/15, Poland

[2] Design & Research Center OKB, 95-006 Brójce, Bukowiec, Rokicińska 108/110, Poland

case of TWCF members subjected to axial compression, a substantial issue is such a design, which promotes a progressive buckling mechanism [1]. However, relatively long thin-walled columns (particularly of open sections) can exhibit additional buckling modes, similar to the Euler buckling, leading to poor energy absorption. Thus, a threshold conditions between progressive buckling and global bending are of crucial importance.

Dynamic buckling response of thin-walled structural members subjected to impact, axial compressive load has been investigated extensively by many researchers. Particularly, closed-section members (tubes) have been investigated since early 60^{ties} of XXth Century. One should mention here Alexander solution for a circular tube and Wierzbicki and Abramowicz works, concerning tubes of prismatic cross-section, quoted by Jones [1]. Those solutions were based on the rigid-perfectly plastic material model and used plastic mechanism approach. They took into account an influence of the strain rate upon the initial material yield stress, but neglected inertia effects. In the contrary to closed-section members, few works have been devoted to the same problem concerning open-section columns. Among them, Kotełko *et al*. [2, 3] published the solution for top-hat section column based on the yield line approach [4], taking into account the strain rate effect. The solution was validated by quasi-dynamic tests, which will be discussed in the next paragraph. Results of experimental investigation of top hat section columns, as well closed section tubes subjected to axial impact were published by Langseth *et al*. [5, 6] and Hsu& Jones [7]. Langseth [6] investigated inertia effect and an influence of impact velocity upon the crushing behaviour of aluminium tubular members.

In recent years some research have been carried out into the transition from progressive local buckling to global bending failure mode in thin-walled columns (bars) under axial impact. Such a transition is observed in the stage of collapse of relatively long bars and at impact velocities higher than a certain ‘critical’ one.

Results, concerning impact behaviour of long, circular and prismatic steel tubes, subjected to dynamic, axial compressive load were bublished by Alves and Karagiosova [8]. They investigated an influence of impact velocity on the crushing behaviour of tubes. The problem of transition from progressive buckling to global bending of circular tubes subjected to axial impact compressive load was also investigated by Alves and Karagiosova [9, 10], as well as Jensen *et al*. [11]. Alves and Karagiosova [10] proposed an analytical model, taking into account inertia effects, which will be discussed in details in 3 paragraph.

Teramoto and Alves [12] conducted research into the same problem for open, channel-section columns subjected to axial impact compressive force. They published results of both experimental tests and FE numerical simulations. They did not find clear condition of the transition from progressive local buckling to global bending.

Determination of ‘limit’ or ‘critical’ values of bar’s length and impact velocity is still an open question. Since a transition from local progressive buckling

to global bending leads to a significant decrease of energy absorption capability, the determination of a threshold criterion between those two failure modes is of crucial importance.

2. QUASI- DYNAMIC BEHAVIOUR

Preliminary static and quasi-dynamic tests have been carried out on relatively short top-hat section and plain channel section columns subject to uniform compression. These tests were conducted in order to plan a program for impact tests and to identify crushing behaviour of open-section columns at relatively low impact velocities. Results of those research was reported by Koteło&Mania [3]. Specimens were made of steel sheets and folded in special folding machine. Dimensions of specimens and material parameters are shown in Table 1. The experiment was conducted on the testing machine Instron of loading range 20 kN. Both compressive force and column deformation (displacement of the upper crosshead beam of the testing machine) was recorded using the integrated, computer aided measurement system of the testing machine.

Table 1

Section	*Material parameters*	*Dimensions*
Top hat 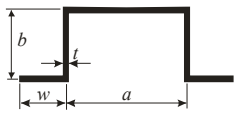	σ_Y = 165 MPa σ_{ult} = 280 MPa E = 192000 MPa E_t = 2000 MPa q = 5 D = 40.4 [1/s]	a = 30 mm b = 30 mm w = 8 mm wall thickness t = 0.6 mm column length l = 150 mm
Plain channel 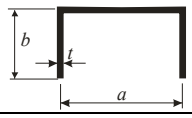	σ_Y= 286 MPa σ_{ult} = 315 MPa E = 194000 MPa E_t = 3000 MPa q, D as above	a = 75 mm b = 37.5 mm wall thickness t = 1 mm column length l = 375 mm

Notation:

E – Young modulus
E_t – tangent modulus
σ_0 – Yield stress
A – area of the cross-section
I – second moment of area of the cross-section
ρ – density of the rod material
m – mass per unit length
L – rod length
G – impactor weight

Figure 1 shows failure modes observed in static and quasi-dynamic tests. Failure modes of top hat sections are significantly different under static and quasi-dynamic load, while failure modes of channel sections did not differ.

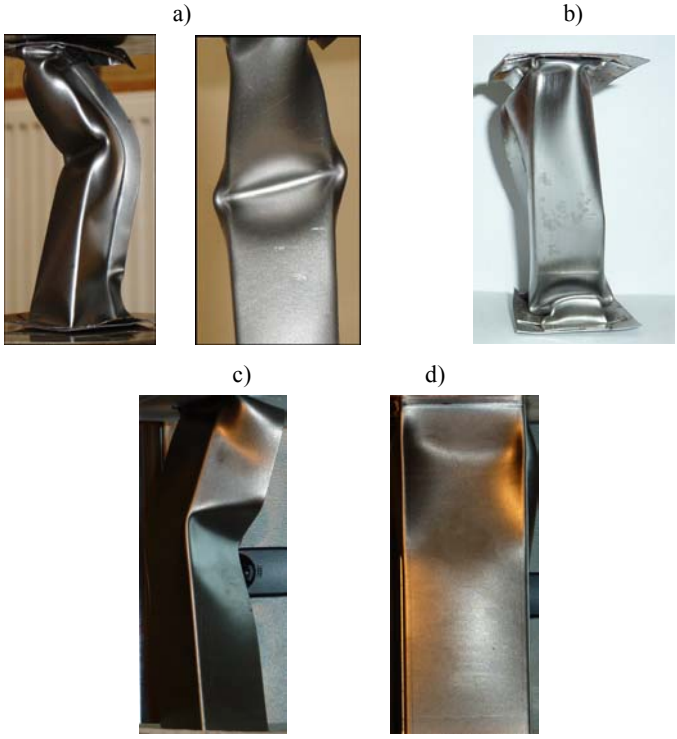

Fig. 1 – Exemplary failure patterns of tested columns: a) top hat –static;
b) top hat $v_0 = 600$ mm/min; c) plain channel $v_0 = 300$ mm/min; d) plain channel $v_0 = 600$ mm/min.

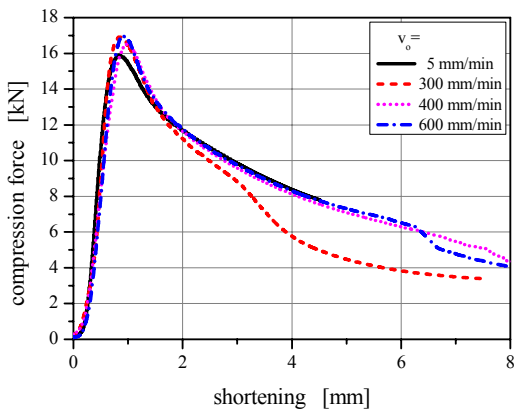

Fig. 2 – Experimental load-shortening diagrams of plain channel sections (quasi-dynamic test).

Experimental quasi-static results show a minor increase of ultimate load due to the increase of loading velocity. Also the failure curves are not significantly influenced by the latter, as shown in Fig. 2 (load-shortening diagrams). That indicates a necessity of actual dynamic crushing tests at much higher impact velocities.

3. ANALYTICAL MODELS

Experiments carried out on axially impacted circular tubes by Alves and Karagiosova [9] and channel – section columns by Teramoto [12] show, that the critical buckling length depends on initial impact velocity and material parameters. Research into analytical solutions of the problem was carried out by Alves and Karagiosova [10], who proposed three theoretical models of dynamic buckling of circular tubes subjected to axial compressive force. There are three different theoretical "rod models" proposed, namely; the Euler buckling model (Fig. 3a), the three-link model (Fig. 3b) and the "two –phase deformation model" taking into account inertia effects and allowing one to analyze an influence of initial velocity on the critical buckling length (Fig. 3c). Generally, it is a model of incompressible rod with uniformly distributed mass $m = M/L$, subjected to the constant axial fully plastic force $P = A\sigma_0$. Since numerous experimental results show, that plastic deformation occurs first near the column ends, in the rod models these deformations are taken into account as "elasto-plastic" bending moments. The models have been derived for the circular tube. Two first models were adopted by Kotełko and Mania [13] for the case of an arbitrary open section column, who presented results of preliminary impact tests of open section members. The last model is also adopted in this work by the authors for an arbitrary case.

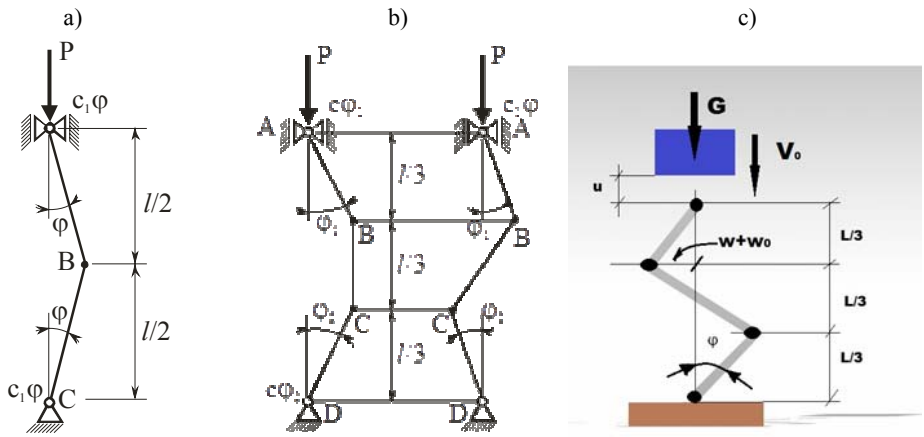

Fig 3 – Collapse modes of "rod" models: a) Euler buckling mode; b) three-link buckling mode; c) two phase deformation model.

In the first case (Fig. 1a) of Euler buckling mode, the equation of motion of each part of the rod (AB and BC), for an arbitrary cross-section, takes the following form:

$$\ddot{\varphi} - \frac{12}{\rho l^2}\left(\sigma_0 - \frac{6E_r I}{Al^2}\right).\varphi = 0, \tag{1}$$

where: $E_r = \dfrac{4E \cdot E_t}{\left(\sqrt{E} + \sqrt{E_t}\right)^2}$ – reduced modulus for bi-linear material [14].

The critical buckling length L_{crE} (Table 2) is an eigenvalue of the equation (1).

Table 2

No	Critical buckling length
1	Euler dynamic buckling mode: $L_{crE} = \sqrt{\dfrac{6E_r I}{A\sigma_0}}$
2	Three-link first dynamic buckling mode: $L^1{}_{cr} = 3\sqrt{\dfrac{E_r I}{A\sigma_0}}$
3	Three-link dynamic second buckling mode: $L^2{}_{cr} = \sqrt{\dfrac{15E_r I}{A\sigma_0}}$

In the second case (Fig. 1b) one can derive four equations of motion (two for each buckling mode) with unknowns φ_1 and φ_2. If the solution of this simultaneous equation is predicted in the following way

$$\varphi_1 = D_1 \sin\left(\omega^2 t + \beta\right) \qquad \omega_2 = D_2 \sin\left(\omega^2 t + \beta\right) \tag{2}$$

the roots of characteristic equation for non-trivial solution are as follows

$$\omega_1^2 = \frac{54}{15mL^3}\left(6c - PL\right); \qquad \omega_2^2 = \frac{5.54}{15mL^3}\left(10c - PL\right), \tag{3}$$

where $c = \dfrac{6E_r I}{\left(1 + \sqrt{\lambda}\right)}$; $\lambda = E_r / E$. The roots of (3) determine two critical buckling lengths for dynamic buckling $L^1{}_{cr}$ and $L^2{}_{cr}$, corresponding to the modes shown in Fig. 1b, given in Table 2.

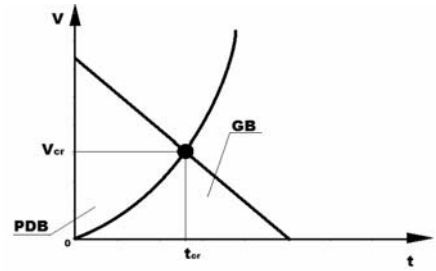

Fig. 4 – Time – velocity diagram.

The third model takes into account inertia effects. The flexure equation of motion takes form:

$$\ddot{w} = \frac{54}{mL^2}\left(L \cdot A \cdot \sigma_0 - 10c\right) \cdot \frac{w}{L} \tag{4}$$

with the solution of a hyperbolic function $w = w_o \cosh(\gamma t)$, where

$$\gamma^2 = \frac{54\left(LA\sigma_0 - 10c\right)}{mL^3}, \tag{4a}$$

γ being an eigenvalue of eq. (4).

The equation of linear motion of the upper end of the rod takes the form:

$$\ddot{u} = 2L \cdot \varphi \cdot \ddot{\varphi} + \dot{\Delta}. \tag{5}$$

Assuming a relation $w = \frac{\varphi L}{3}$, we can derive the velocity of the upper end of the rod $\dot{u}$ as follows:

$$v_1 = \frac{9w_0^2 \cdot \gamma}{} \sinh\left(\gamma t\right). \tag{6}$$

On the other hand, the equation of the motion of the impactor is as follows:

$$G\dot{v} = -A\sigma_0 \tag{7}$$

and, subsequently the velocity of the impactor amounts:

$$v = v_0 - \frac{A}{G}\sigma_0 t\,. \tag{8}$$

Comparing the velocity of the impactor (8) with the velocity of the impacted end of the rod (9), we obtain a transcendent equation:

$$v_0 - \frac{A}{G}\sigma_0 \cdot t = \frac{9w_0^2}{L}\sinh\left(\gamma t\right), \tag{9}$$

with the root (t_{cr}), a critical instant, at which a transition from progressive local buckling to global bending takes place (Fig. 4). A corresponding critical velocity is as follows:

$$v_{cr} = v_0 - \frac{A}{G}\sigma_0 t_{cr} . \tag{10}$$

The values of t_{cr} and v_{cr}, corresponding to relations (9) and (10) are given in Table 5.

4. DYNAMIC IMPACT TESTS

4.1. TESTING PROGRAM

The testing program for impact tests was planned in the way, which allowed one to observe the transition from local progressive buckling to global bending failure mode at certain critical lengths and velocities. Thus, dimensions of specimens to be tested were determined in order to assure local buckling under static load. Omn the other extreme, lengths of specimens were taken to be slightly less and slightly greater than critical values, calculated on the basis of theoretical models discussed in paragraph 3.

The dimensions of specimens (columns), which have been tested are shown in Table 3. Two series of columns have been tested: series "**1**" – plain channel and series "**2**" – top hat section. Impact tests were carried out on steel specimens of different a/b ratio and different length from 250 to 500 [mm]. Wall thickness of all columns was $t = 1$ mm.

The specimens were made of steel sheets. Standard tensile tests were performed on coupons cut from the sheet (row material). Material properties determined were as follows:

– Yield stress $\sigma_0 = 201.5$ MPa

– Young modulus $E = 1.75 \cdot 10^5$ MPa

– tangent modulus $E_t = 2000$ MPa.

Similarly to the specimens made for quasi-dynamic tests, steel sheets were folded in folding machine. All rolling radii were of the same magnitude $r = 2.5$ mm.

All specimens were clamped in two parallel plates (situated in grooves made by milling machine) and spot welded , as shown in Fig. 7.

Table 4 shows main parameters and critical lengths of specimens, calculated according to two first theoretical models (pos. 1–3 Table 2) for sections under investigation.

Alltogether about 90 impact tests were carried out at different impact velocities from 4 to 10 [m/s] and impact energy up to 4.5 kJ.

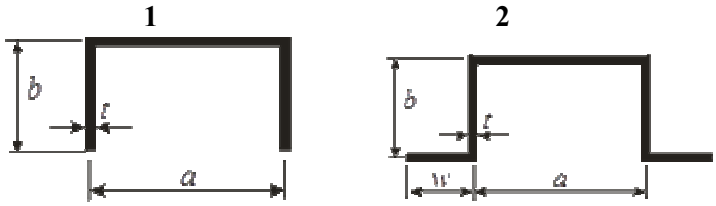

Fig. 5 – Tested sections: 1 – plain channel, 2 – top hat.

Table 3

Symbol	*a* [mm]	*b* [mm]	*w* [mm]	Length *L* [mm]
A1	60	60	-	250
A1	60	60	-	300
A1	60	60	-	400
A1	60	60	-	500
B1	90	45	-	200
B1	90	45	-	300
B1	45	90	-	350/400
D1	60	45	-	250
D1	60	45	-	300
D1	60	45	-	400
D1	60	45	-	500
D2	60	45	15	250
D2	60	45	15	300
D2	60	45	15	400
D2	60	45	15	500

Table 4

Symbol	*a* mm	*b* mm	*w* mm	*A* mm^2	$A\sigma_0$ N	L_{crE}	L_{cr}^1	L_{cr}^2
A1	60	60	-	187.8	37841.7	**291**	**356**	**460**
B1	90	45	-	187.8	37841.7	**215**	**263**	**339**
D1	60	45	-	157.8	31796.7	**220**	**269**	**348**
D2	60	45	15	195.6	39413.4	**278**	**341**	**440**

4.2. EXPERIMENTAL STAND

Experiments were carried out on the drop hammer rig (Fig. 6), which consists of the impactor of changeable mass (2) , hoisting mechanism and release mechanism of the hammer (4,5) as well as additional springs (3), which allow one to increase the energy of impact. The springs are driven by the separate driving system. All mechanisms are controlled by a special computer program. The measuring system consists of piezoelectric force transducer, situated at the bottom of the specimen (1), displacement transducer and accelerometer.

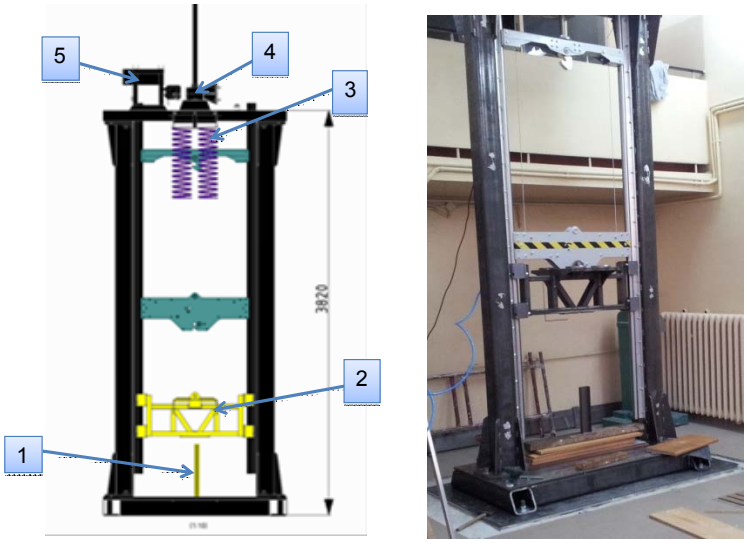

Fig. 6 – Drop hammer rig general view.

Fig. 7 – Drop hammer rig: specimen's lay-out.

4.3. TEST RESULTS

As was mentioned above, altogether about 90 impact tests were conducted under different impact velocities from 4.5 to 10 [m/s]. Results of tests carried out on the specimens of the same dimensions and under the same testing conditions were repeatable.

The summary of the results of tests is given in Table 5. Theoretical values of critical instant and corresponding critical velocity calculated according to the model III – par. 3, relations (9, 10) are shown in last two columns.

The results of the tests were partially in agreement with analytical models I and II. For 14 of the examined cross-sections the observed failure mode was in good

agreement with the theoretical one. In 9 cases of the tested cross-sections a transition from local progressive dynamic buckling (PDB) to global bending failure mode (GB) was observed for columns of lengths, which corresponded to intervals of critical lengths coming from analytical models I and II. It concerned plain channel sections.

In the case of top hat sections only the progressive buckling failure mode was observed, additionally, in some cases, an interaction of progressive buckling and flexural-torsional buckling was recorded.

In the case of IIIrd analytical model, the calculated critical time intervals were larger than the actual total time of impact (Fig. 9).

Table 6 shows failure patterns of all examined columns, corresponding to Table 5. In Figs. 8 and 9 exemplary failure modes are presented in details. Fig. 8 shows a difference in failure patterns of three columns of the same dimensions of the cross-section and length, subjected to different impact velocities. As one can notice, the difference is significant. In Fig. 9 the transition from progressive dynamic local buckling to global bending failure mode is presented for tewo columns of the same cros-section dimensions and different length: $L < L_{crE}$ (Fig. 9a) and $L_{cr1} < L < L_{cr2}$ (Fig. 9b). Failure mode in Fig. 9b corresponds to II. theoretical model, namely three-link model.

Table 5

Sp. No	Symbol	Dimensions	Energy/velocity	Failure mode	Notes	t_{cr}^*	V_{cr}^*
		***a* / *b* /*w* / *L* [mm]**	**[kJ] / [m/s]**	**-**	**-**	**[s]**	**[m/s]**
1	A1	60/60/-/250	2/8.94	**PDB**$^{(*)}$	$L<L_{crE}$		
2	A1	60/60/-/250	1/6.32	**PDB**	$L<L_{crE}$		
3	A1	60/60/-/250	0.5/4.47	**PDB**	$L<L_{crE}$		
4	A1	60/60/-/300	1/6.32	**PDB**	$L_{crE}<L<L_{cr1}$	0.20	6.16
5	A1	60/60/-/300	0.5/4.47	**PDB**	$L_{crE}<L<L_{cr1}$	0.19	4.32
6	A1	60/60/-/400	1/6.32	**PDB**	$L_{crE}<L<L_{cr2}$	0.19	6.18
7	A1	60/60/-/400	0.5/4.47	**GB**$^{(**)}$	$L_{crE}<L<L_{cr2}$	0.18	4.33
8	A1	60/60/-/500	1/6.32	**PDB**	$L>L_{cr2}$	0.21	6.16
9	B1	90/45/-/200	1.5/7.75	**PDB**	$L<L_{crE}$		
10	B1	90/45/-/300	1.5/7.75	**GB**	$L_{cr1}<L<L_{cr2}$	0.13	7.65
11	B1	90/45/-/400	1.5/7.75	**GB**	$L>L_{cr2}$	0.16	7.63
12	D1	60/45/15 -/250	1.5/7.75	**GB**	$L_{crE}<L<L_{cr1}$	0.13	7.65
14	D1	60/45/-/250	1.5/7.75	**PDB**	$L<L_{crE}$		
15	D1	60/45/-/250	1.5/7.75	**GB**	$L_{crE}<L<L_{cr1}$	0.13	7.66
16	D1	60/45/-/300	1.5/7.75	**GB**	$L_{cr1}<L<L_{cr2}$	0.14	7.66
17	D1	60/45/-/300	1/6.32	**GB**	$L_{cr1}<L<L_{cr2}$	0.13	6.24
19	D1	60/45/-/400	1.5/7.75	**GB**	$L>L_{cr2}$	0.16	7.65
20	D1	60/45/-/400	1/6.32	**PDB**	$L>L_{cr2}$	0.16	6.22
21	D1	60/45/-/500	1/6.32	**GB**	$L>L_{cr2}$	0.2	6.119
22	D2	60/45/15/250	1/6.32	**PDB**	$L<L_{cr}$		
23	D2	60/45/15/300	1/6.32	**PDB**	$L_{crE}<L<L_{cr1}$	0.18	6.18
24	D2	60/45/15/400	1/6.32	**PDB**	$L_{cr1}<L<L_{cr2}$	0.18	6.18
25	D2	60/45/15/500	1/6.32	**PDB**	$L>L_{cr2}$	0.21	6.16
13	D2	60/45/-/250	1.5/7.75	**PDB**	$L<LcrE$	0.38	7.44
18	D2	60/45/15/400	2.2/9.38	**PDB**	$L_{cr1}<L<L_{cr2}$	0.18	9.24

$^{(*)}$ progressive dynamic local buckling, $^{(**)}$ global bending

Table 6

1	**2**	**3**	**4**	**5**
6	7	8	9	10
11	12	14	15	16
17	**19**	**20**	**21**	**22**
23	**24**	**25**	**13**	**18**

a) **b)** **c)**

Fig. 8 – Column A1, L= 250 mm: a) v_0 = 4.47 m/s; b) v_0 = 6.32 m/s; c) v_0 = 8.94 m/s.

a) b)

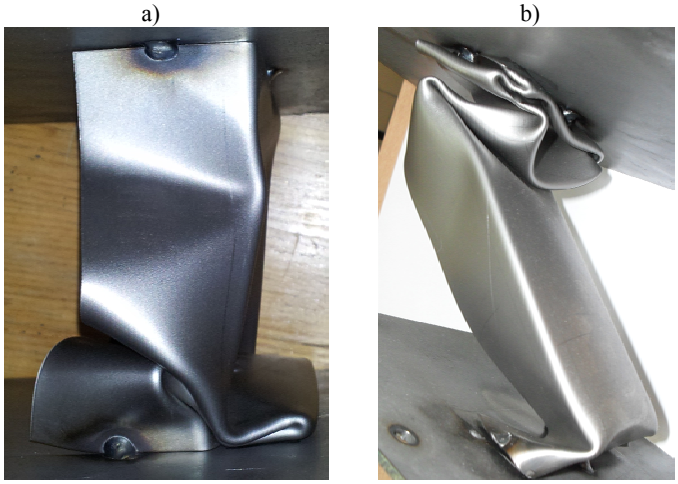

Fig. 9 – Column B1, v_0 = 7.75 m/s: a) L = 200 mm (No 9); b) L = 300 mm (No 10).

a) b)

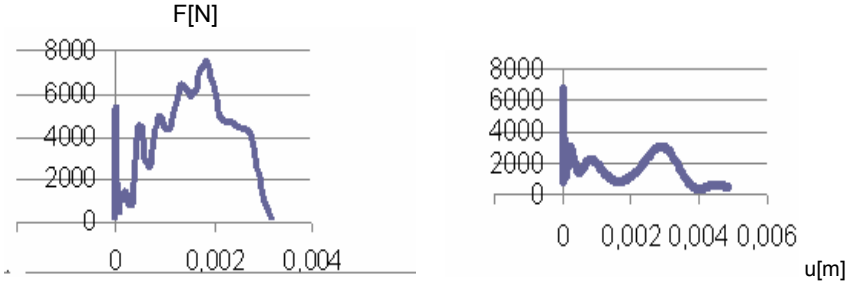

Fig. 10 – Load-shortening diagrams: column B1, v_0 = 7.75 m/s: a) L = 200 mm (No 9); b) L = 300 mm (No 10).

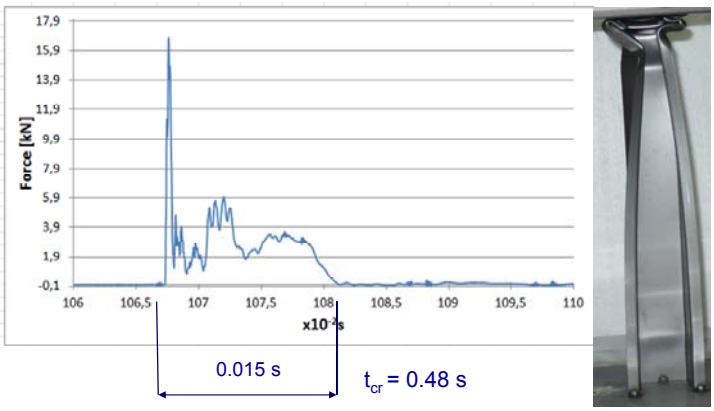

Fig. 11 – Column D2, L = 500 mm, v_0 = 6.32 m/s (25).

Load-shortening diagrams for columns shown in Fig. 9a and 9b are presented in are presented in Figs. 10a and 10b, respectively. The diagrams indicate, that a global bending failure mode of the column of length $L > L_{cr}$ leads to a poorer energy absorption capacity. An exemplary load-time for top-hat section column is shown in Fig. 11a, while Fig. 11b presents the typical failure mode for the longest top-hat section column, for which local dynamic buckling was observed.

5. CONCLUSIONS

The "rod" models proposed by Alves and Karagiosova [10] occurred to be not entirely adequate for open section members. However, the critical buckling length for dynamic buckling, calculated on the basis of the I. and II. model, was in relatively good agreement with the results of experiments in several cases of plain channels. Thus, those simple analytical models may be useful in prediction of crushing behaviour of channel section columns, particularly at the preliminary stage of design process.

In nearly all examined cases, critical time intervals, calculated according to IIIrd two-phase theoretical model , taking into account inertia effects, for which a transition should take place, were larger than the total actual time of impact.

In the case of top hat sections only the progressive buckling failure mode was observed. It is probably induced by the edge stiffeners, which stabilize the column during impact.

More clear indications of the threshold criterion (or criteria) of the transition between progressive buckling and global bending can be obtained from further research which would take into account larger diversity of impact velocities and dimensions. Also impact tests at different impact mass have to be performed in order to investigate inertia effects.

Simultaneously with experiments reported in this paper, numerical FE simulations were carried out and are in progress. Results of those numerical experiments, which will be presented in a separate publication will deliver a more clear understanding into the phenomenon of transition between progressive buckling and global bending of open section members subjected to axial, impact compressive force.

Received on: July 16, 2014

REFERENCES

1. JONES, N. *Structural Impact*, Cambridge University Press, 2003.
2. KOTEŁKO,M, MANIA, R., KOŁAKOWSKI, Z., *Dynamic crushing of thin-walled profiles*, Proc. of ICTWS Conference "Thin-walled Structures-Recent Innovations and Developments", ed. by M. Mahendran, Queensland University of Technology, Brisbane, June 2008, pp. 687–693.

3 KOTEŁKO M., MANIA R.J.: *Quasi-static and dynamic axial crushing of TWCF open-section members*, Int. Journal of Thin-Walled Strc., **61**, pp. 115–120, 2012.
4. KOTEŁKO M. *et al*., *Plastic mechanisms database for thin-walled cold-formed steel members in compression and bending*, Thin-Walled Structures, **48**, pp. 818–826, 2010.
5. LANGSETH M. *et al*., *Crash behaviour of thin-walled aluminium members*, Thin -Walled Struct., **32**, pp. 127–150, 1998.
6. LANGSETH M. *et al*., *Crashworthiness of aluminium extrusions. Validattion of numerical simulation. Effect of mass ratio and impact velocity*, Int. J. Impact Eng., **22**, pp. 829–854, 1999.
7. HSU S.S., JONES N., *Dynamic axial crushing of circular and square stainless steel tubes. Structures under shock and impact*, VII, pod red. Jonesa i in. WIT Press, 2001, pp. 169–178.
8. ALVES M. KARAGIOSOVA D*., Influence of the Arial impast velocity on the buckling behaviour of circular cylindrical shells*, Proc. of 9th National Congress on Theoretical and Applied Mechanics, Demetra Ltd., Bulgaria, 2001, pp. 388–393.
9. ALVES M. KARAGIOSOVA D., *Transition from progressive buckling to global bending of circular shells under axial impact – Part I: Experimental and numerical observations*, Int. J. of Solids and Struct., **41**, pp. 1565–1580, 2004.
10. ALVES M. KARAGIOSOVA D., *Transition from progressive buckling to global bending of circular shells under axial impact – Part II: Mathematical model*, Int. J. of Solids and Struct., **41**, 2004, pp. 1581–1604.
11. JENSEN O. *et al.*, *Transition between progressive and global buckling of aluminium Extrusions*, in: *Structures under shock and impact*, VII, Ed. by N. Jones, WIT Press, Southhampton, Boston, 2002, pp. 269–277.
12. TERAMOTO S.S., ALVES M., *Buckling transition of axially impacted open shells*, Int. J. of Impact Eng., **30**, 2004, pp. 124–126.
13. KOTEŁKO M., MANIA R.J., *Investigation into different collapse modes of twcf open section members under axial impact*, Proc. of ICTWS'2012, Glasgow , pp.391–399, 2012.
14. WIERZBICKI T., SINMAO N.W., *A simplified model of Brazier effect in plastik bending of tubes*, Int. Journal of Pressure Vessels, **71,** *1*, pp. 19–28, 1997.